

Exploring the ENEA Casaccia and ENEA Frascati irradiation capabilities: Status and perspectives

Michele Croia^{1,*}, Nunzio Burgio¹, Alessandro Ampollini², Maria Denise Astorino², Giulia Bazzano², Barbara Bianchi¹, Mateo Cesaroni¹, Luca Falconi¹, Salvatore Fiore^{2,3}, Luigi Lepore¹, Augusto Nascetti⁴, Paolo Nenzi², Antonino Pietropaolo², Concetta Ronsivalle², Alfonso Santagata¹, Antonino Ratto¹, Pierpaolo Ricci¹ and Luigi Scaramuzzo¹

¹ENEA Casaccia research center, Rome, Italy

²ENEA Frascati research center, Frascati, Italy

³CERN, Geneva, Switzerland

⁴School of Aerospace Engineering, Sapienza University of Rome, Italy
(*) michele.croia@enea.it

Abstract—A collaboration between different facilities in Casaccia and Frascati ENEA research centers has recently opened the possibility of performing irradiation experiments using different kinds of particles such as protons, neutrons, and electrons. The facilities involved in the project are the TAPIRO fast nuclear research reactor, the TOP-IMPLART proton accelerator (71 MeV), the REX electron accelerator (5 MeV) and the FNG neutron facility (2.5/14 MeV). This suite of plans represents a distributed irradiation facility using different particles and spectra, offering various irradiation capabilities for experiments in many fields, such as: nuclear physics, accelerator physics, aerospace, science material, medicine, detectors, radiation diagnostics, etc. Complete numerical models of all the facilities have been implemented to perform start-to-end simulations before experimental irradiation using beam dynamics and nuclear transport simulation codes. In addition, our distributed irradiation facility makes it possible to recreate an essential part of the Van Allen Belt radiation allowing us to check the FLUKA quantitative calibration regarding this specific simulation, facilitating the disentanglements of the uncertainties. Finally, a comparison of the estimated silicon 1 MeV neutron equivalent fluence (SIIMEVNE) of the radiation damage imparted by the different facilities is presented.

Keywords —Nuclear research reactor, Particle accelerator physics, Neutron generator, Irradiation Facility, Aerospace, Science material, Beam dynamics, Monte Carlo simulations.

I. INTRODUCTION

HISTORICALLY, ENEA nuclear irradiation facilities were involved, during the years, in activities related to material sciences, Gen IV nuclear reactors, Accelerator Driven Systems (ADS), Nuclear Fusion, Medical Isotope production and radiotherapy, qualification of radiation-hardened electronic components, nuclear detector calibration, radio-dosimetry. Up to date, these laboratories have worked on the above-cited activities in parallel into separate tasks, without needing to be directly connected. However, the need to design complex components and test them against a complex mixed radiation

field, such as aerospace systems, poses the question of ascertaining the representativeness limits of the ENEA facilities of the radiative spatial condition. An example of the practical representation of the Van Allen Belt complex orbital radiation field at 5830 km to be used in design activities is given in [1]. All experiments or tests that must be conducted in these environments require as much as possible the creation of the same multi-particle radioactive environment, covering as many energy spectra as possible.

The task of artificially reproducing these radioactive environments is entrusted to irradiation facilities (nuclear research reactors, particle accelerators, radioactive sources), which allow for the irradiation of experimental samples subjected to a limited number of types of radiation and energy spectra. Regarding the neutron energy spectrum, nuclear reactors can generate a thermal spectrum or a fast spectrum essentially depending on the moderator used [2]. For particle bunches or ions produced via particle accelerators the final spectra depend on the accelerator itself i.e., accelerator length and accelerating gradient.

In some facilities it is possible to reproduce an environment consisting of multi-particle radiation. Typically, this is a bunch of primary particles impinging on an appropriate target to produce secondary radiation. This is what happens in the neutron and muon sources [3-6].

Our collaboration between different facilities within the same institute has created a Distributed Facility for multi-particle irradiation, which allows irradiation experiments with different types of radiation (neutrons, protons, and electrons) and different energy spectra. One of the main advantages of the distributed facility is therefore the simplicity of access for the user who needs to irradiate a sample to be subjected to a radioactive environment using particles of different nature.

The aim of this work is to introduce the design of a simple irradiation experiment having the scope to demonstrate the feasibility of the ENEA distributed facility for aerospace investigation. In the following, after the presentation of each single irradiation facility participating in the distributed system, we present a simple one-unit CubeSat layout that has a dosimeter as payload. Based on the simulation outcomes, we

establish that the distributed facility has the capability to cover the trapped particles and the solar energetic particle emission energy range with the exclusion of the Galactic Cosmic Rays (GCR) contribution. The simulation tuning, based on the MCNP and FLUKA codes, has been performed using as input the outcomes from beam dynamics codes for the particle accelerators and nuclear properties of the research nuclear reactor. As a reference, we used the experimental data obtained from the ABCS satellite that was launched into orbit in the Van Allen belt (5860 km of altitude) in 2022 [1].

II. THE DISTRIBUTED IRRADIATION FACILITY

The ENEA Distributed Irradiation facility is composed by four different devices: the RSV TAPIRO nuclear research reactor, the Frascati Neutron Generator (FNG), the TOP-IMPLART proton linac accelerator and the REX electron linac accelerator.

A. The RSV TAPIRO fast nuclear research reactor

RSV TAPIRO (Reattore Sorgente Veloce - TARatura Pila Rapida a Potenza 0 - Fast Pile Calibration at 0 Power) is a source of neutrons generated in the fission process in a highly enriched Uranium-Molybdenum alloy. Depending on the irradiation position inside the nuclear reactor, different neutrons' energy distributions, and intensities are used to satisfy the experiments' needs. The almost fission energy spectrum is available in the core center with a neutron flux intensity of $4 \times 10^{12} \text{ cm}^{-2}/\text{s}^{-1}$ at the maximum power of 5 kW. In the other irradiation channels, less energetic neutrons are usable up to epithermal and thermal neutrons in the Thermal Column Cavity (TCC). A detailed description of the reactor and possible applications are in [7]. Fig. 1 shows the RSV TAPIRO schematic layout, with experimental channels indicated.

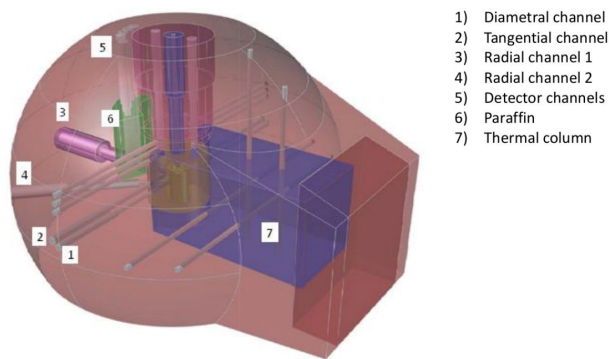


Fig. 1 Schematic layout of the RSV TAPIRO nuclear research reactor and its experimental channels.

B. The Frascati Neutron Generator – FNG

The Frascati Neutron Generator (FNG) is a compact accelerator driven neutron source installed and operating at the ENEA Frascati Research Centre, thoroughly described in [8,9,10]. It relies on both Deuteron-Deuteron (D-D) and Deuteron-Tritium (D-T) fusion reactions, in turn producing almost monochromatic 2.5 MeV and 14 MeV neutrons with a maximum neutron emission rate up to 10^9 s^{-1} and up to 10^{11} s^{-1} ,

respectively. Fig.2 shows a schematic 3D representation of FNG.

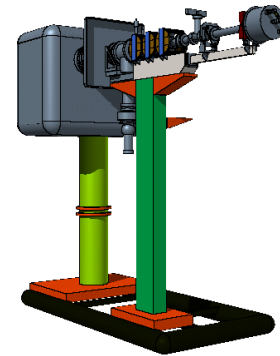


Fig. 2 Schematic layout of the FNG facility.

In D-T mode, the source neutron emission rate is determined by means of an absolute measurement, the so-called associated alpha particle technique [11]. Simulations, benchmarked by means of experimental measurements, provide a neutron yield and flux determination within an uncertainty of 3% [8,9,10]. In D-D mode the 2.5 MeV neutron emission rate is determined using foil activation technique, where a ^{115}In is irradiated and the gamma activation following the $^{115}\text{In} (n,n') ^{115}\text{In}_m$ reaction channel is measured by means of an absolutely energy calibrated High-Purity Germanium detector. The D-D neutron emission is measured at $\pm 7\%$ uncertainty.

C. The TOP-IMPLART proton linac

The TOP-IMPLART particle accelerator [12] is a technology demonstrator of a pulsed, fully linear machine for proton therapy under development at ENEA Frascati Research Centre in collaboration with the Italian Institute of Health (ISS) and the Oncological Hospital Regina Elena-IFO. It is a unique and compact accelerator, exploiting S-band accelerating structures from energies as low as 7 MeV, and one of the few proton sources above 60 MeV available in Italy. It comprises a commercial injector, by ACCSYS-Hitachi, and 8 Side Coupled DTL structures, patented by ENEA, accelerating the proton beam to a maximum energy of 71 MeV and maximum intensities of 4.5×10^8 protons per pulse. A set of two scanning magnets allow irradiation of an area up to $10 \text{ cm} \times 10 \text{ cm}$. Fig. 3 shows a schematic layout of the accelerating line, from the injector up to reach the final energy of 71 MeV.

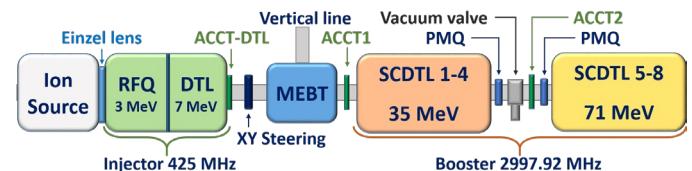


Fig. 3 Layout of the TOP-IMPLART accelerating line. The first extracting point is in the vertical line (7 MeV.) At the end of the entire line (71 MeV) are located the two scanning magnets.

Table I reports the main accelerators and beam parameters at the end of the linac, before the two scanning magnets.

TABLE I
 TOP-IMPLART FINAL PARAMETERS

Quantity	Final values
Pulse length	2.4 μ s
Pulse repetition frequency	25 Hz
Protons per pulse (max)	4.5×10^8
Pristine energy on target	61 – 70 MeV
Pencil beam spot size (FWHM)	17 mm
Maximum proton flux on a 10 cm \times 10 cm area	1.1×10^8 cm ⁻² s ⁻¹

Main parameters for the irradiations at the end of the accelerator line.

D. The REX electron linac.

The REX irradiation facility [13] operating at ENEA Frascati Research Center is based on a 5 MeV S-band on-axis coupled electron linear accelerator. It can provide two types of radiation: electrons and photons. It is equipped with a removable conversion unit for secondary X-Ray emission, generated by bremsstrahlung from the 5 MeV electron beam. The irradiation chamber (dimensions: 40cm x 40cm x 80cm) can be equipped with a remote positioning system to scan the specimens for complete exposure to the beams. Fig.4 shows the schematic layout of the accelerator and the irradiation chamber.

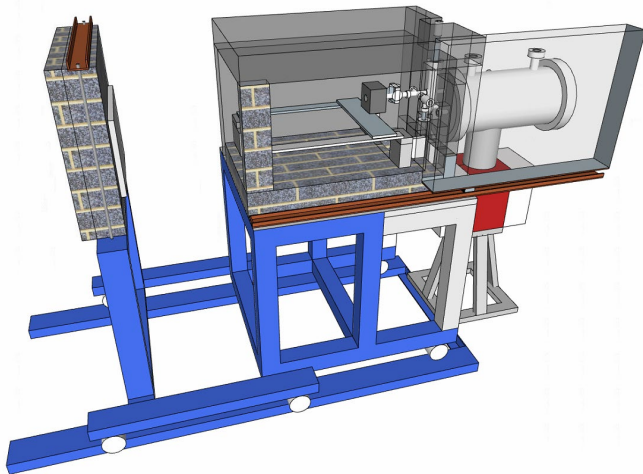


Fig. 4 Schematic layout of the REX accelerator and of the irradiation chamber.

In Table II are reported the main REX beam parameters.

TABLE II
 REX FINAL PARAMETERS

Quantity	Final values
Pulse duration	3 μ s
Electron per pulse (max)	2.95×10^{12}
Pristine energy on target	5 MeV
Spot size 5cm from the linac exit (FWHM)	20 mm
Pulse current (max)	150 mA
Average current	9 μ A
Electrons per second (max)	5.6×10^{13} s ⁻¹

Main parameters at the end of the accelerator line.

III. IRRADIATION OF A SATELLITE IN THE DISTRIBUTED FACILITY TO PARTIALLY RECREATE THE VAN ALLEN BELT RADIATION CONDITIONS

The Astro Bio CubeSat (ABCS) was launched in the Van Allen belt [1] in July 2022, in a period of Solar maximum activity that triggered a Coronal Mass Ejection, causing the arrival of high flux Solar Energetic Particles (SEP) in the proximity of the Earth. After seven days of the mission, the satellite data transmission to Earth suddenly ceased, and the causes are currently under investigation.

However, the first two mission days completed all the experimental activities concerning the onboard multi-analytical platform. Also, an exhaustive data flow on the dose measures within the payload was received. The measured cumulative dose time evolution within the payload obtained by the onboard metal-oxide-silicon Field-Effect Transistors radFET [14], oscillates but its trend increases almost linearly, fitting the data it is possible to quantify the dose in 7.7 rad/day [14], that seems to confirm that the satellite was only marginally irradiated by the SEP.

Comparing the measured integral dose with the one simulated using FLUKA (FLUktuierende KAskade) Monte Carlo code [15], assuming a very poor SEP contribution to the dose along the orbit, we found an initial difference of 27% [16] that refining the calculation was lowered to 1.89% [17]. To verify, the simulated radFET answer, we will measure the dosimeter response using the distributed irradiation facility. The program for the irradiation consists firstly in the implementation of a CubeSat-like unit with a payload shell hosting the same radFET dose counter used in the ABCS mission, a VARADIS VT02 [18]. We already built the satellite shell. Fig. 5 shows a copy of the CubeSat that was produced by T.S.C [19], recreating the same technical features used in the ABCS mission.



Fig. 5 One of the copies that we realized for the irradiations. Inside it is visible a housing for placing the electronic board containing the radFET. A 2mm thick hole was made in one of the walls to allow for the possible passage of cables during the irradiation.

By means of FLUKA simulations, we evaluated the material activation during and after the irradiations in all the facilities. The shell, as in the mission, was realized in an anticorrosive alloy, this will allow to extract and handling in a relatively short time the CubeSat unit, even after the irradiation with neutrons.

Currently, we are implementing the electronic board to insert in the CubeSat unit. The information collected during the irradiation will be also useful to establish the general irradiation protocol of a full replica of the ABCS.

The second step of the program before the irradiations foresees complete Start-to-End (S2E) simulations for each facility. The last step will be the irradiations to measure the components' response comparing experimental results with simulations outcomes.

IV. SIMULATIONS OF THE IRRADIATIONS

The facility covers an interval of energies with different kinds of particles (neutrons, protons, electrons, and gammas) and can be used in parallel to investigate the impact of mixed field radiations. In Table III there are the flux intensities, their abundance, and mean energies of the energy distribution of the primary orbital source term in ABCS orbit. The values show that we are almost representative of the Van Allen belt radiative environment.

TABLE III
PARAMETERS IN THE ABCS ORBIT

	Flux intensity ($\text{cm}^{-2}\text{s}^{-1}$)	Worth (%)	Flux weighted energy (MeV)
Trapped protons	5.9×10^6	6.31	2.884×10^{-1}
<i>GCR protons</i>	8.8	9×10^{-6}	576.71
<i>SEP protons</i>	5.7×10^5	6.03×10^{-1}	1.501
<i>Trapped electron</i>	8.7×10^7	93.09	1.409×10^{-1}
<i>Total</i>	9.4×10^7	100	

Trapped protons and SEP protons have flux weighted energies covered by the 70 MeV protons of TOP_IMPLART while REX electron accelerator covers the trapped electron mean flux. GCR protons flux weighted energy outperforms the TOP_IMPLART energy range.

A. Simulated proton beam irradiation @ TOP_IMPLART

To perform S2E simulations we simulated the beam from the injector up to the interaction point. The simulated beam parameters at the interaction point are a spot size of $\sigma_{x,fwhm}=1.7$ cm, a medium (peak) current of $\bar{I}(I) = 1.2 \mu\text{A}$ (20 mA), a final beam energy of $E \approx 70$ MeV.

To simulate the interaction between the proton bunch and the CubeSat we used FLUKA, in which we modeled the CubeSat structure, and we used as input the proton beam parameters from the beam dynamics simulations. Fig. 6 shows a cross-section of the CubeSat geometry having superimposed the integral mesh of the estimated energy density in $\text{GeV cm}^{-3} \text{nA}^{-1}$, normalized at 1 nA obtained in the simulated irradiation at TOP_IMPLART, in the central part of the satellite is located the card containing the radFET.

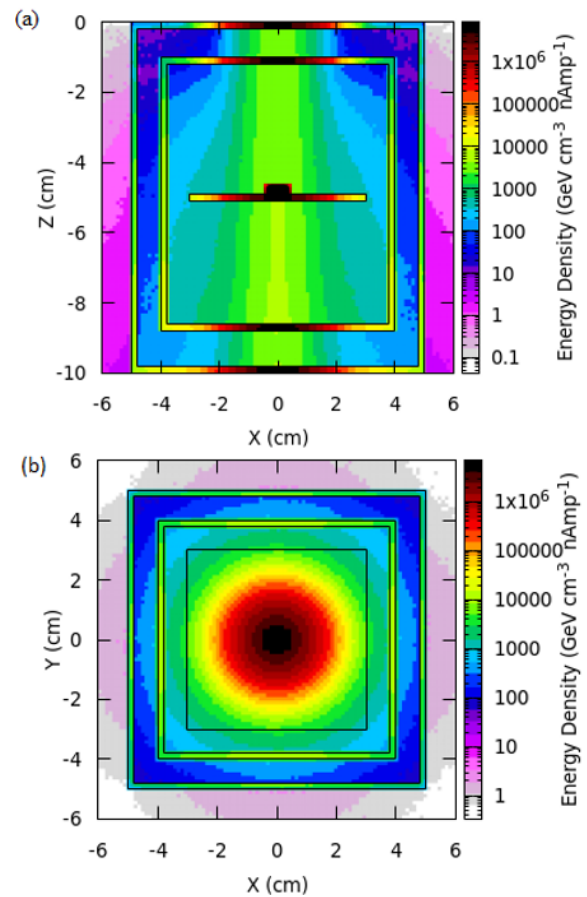


Fig. 6 Simulated energy deposition of the proton beam on the CubeSat. 6. (a) Axial view of the irradiation, in the upper part of the figure the beam from TOP_IMPLART penetrates the satellite. The loss of energy and the widening of the beam is clearly visible. 6. (b) Radial view of the energy deposition.

B. Simulated electron beam irradiation @REX

Using the same procedure, we simulated the interaction between the electron bunch from the REX accelerator and the CubeSat. Using beam dynamics simulation codes, we obtained the beam parameters at the interaction point: a spot size of $\sigma_{x,fwhm}=3.8$ cm, a medium (peak) current of $\bar{I}(I) = 9 \mu\text{A}$ (150 mA), a final beam energy of $E \approx 5$ MeV. Implementing the beam parameters in FLUKA we simulated the interaction between accelerated electrons and the dummy satellite. Fig. 7 shows the estimated axial and radial deposited energy densities normalized per μA ($\text{GeV cm}^{-3} \mu\text{A}^{-1}$).

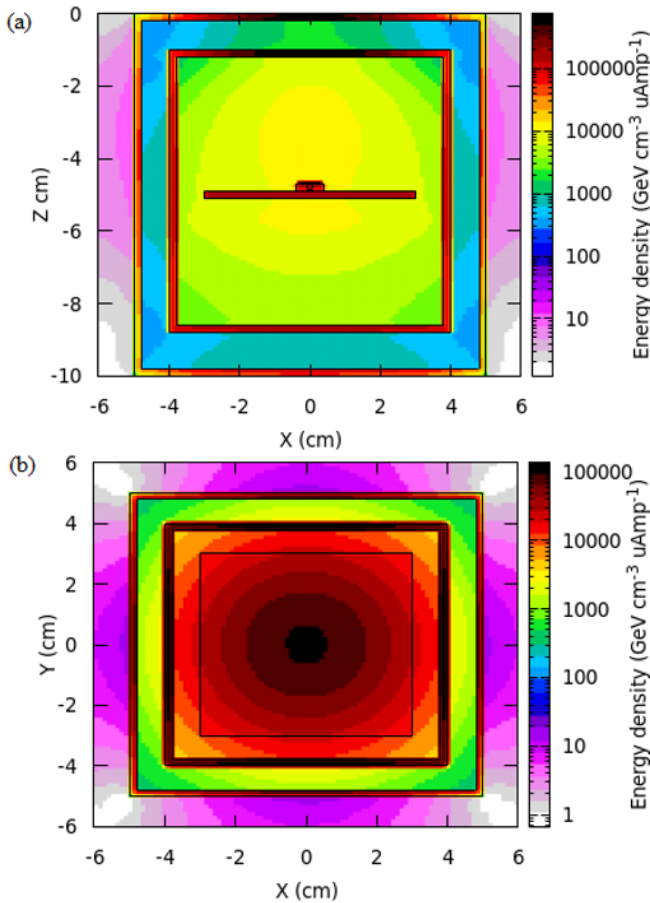


Fig. 7 Simulated energy deposition of the electron beam on the CubeSat. Fig. 7. (a) Top view of the irradiation, in the upper part of the figure the beam from REX penetrates the satellite. The loss of energy and the widening of the beam is clearly visible. 6. (b) Front view of the irradiation. The view shows the integral of the simulated interaction.

C. Irradiation with neutrons @TAPIRO

Fig. 9 reports the geometrical cross-section of the MCNP TAPIRO model [20] showing the irradiation position inside the TCC in which we simulated the irradiation of the CubeSat-like structure within the TCC intending to estimate its performance in terms of equivalent damage (S1MEVNE). By comparing such simulation outcomes with the equivalent damage estimated for the orbital source, we can estimate the effectiveness of the neutrons as a source of damages. A similar estimation has been already carried out in [1] for the whole ABCS structure.

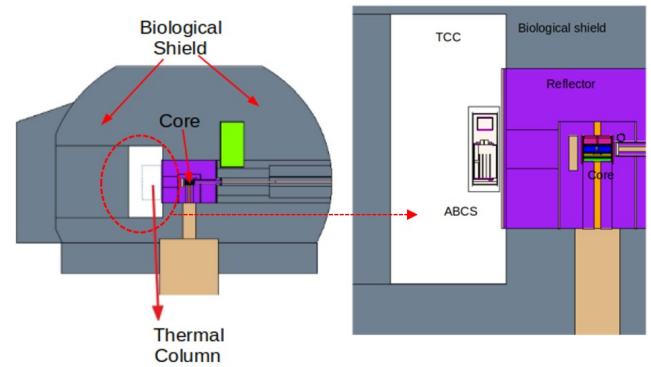


Fig. 9 Cross-section of the TAPIRO MCNP model layout. The left part of the figure reports the Thermal Column Cavity (TCC), the neutron reflector, the core, the radial channel, and the biological shield. The right part reports a magnification of the TCC, where is reported a section of the full ABCS model.

D. Irradiation with neutrons @FNG

For the scope of the present FLUKA simulation, we considered only the forward neutron flux generated by FNG in D-T mode (source emission rate $1 \times 10^9 \text{ s}^{-1}$). Fig. 8 reports the distribution of the energy deposited along the CubeSat structure. More detailed modelling of the D-T neutron source will be implemented in the next phase of experimental design.

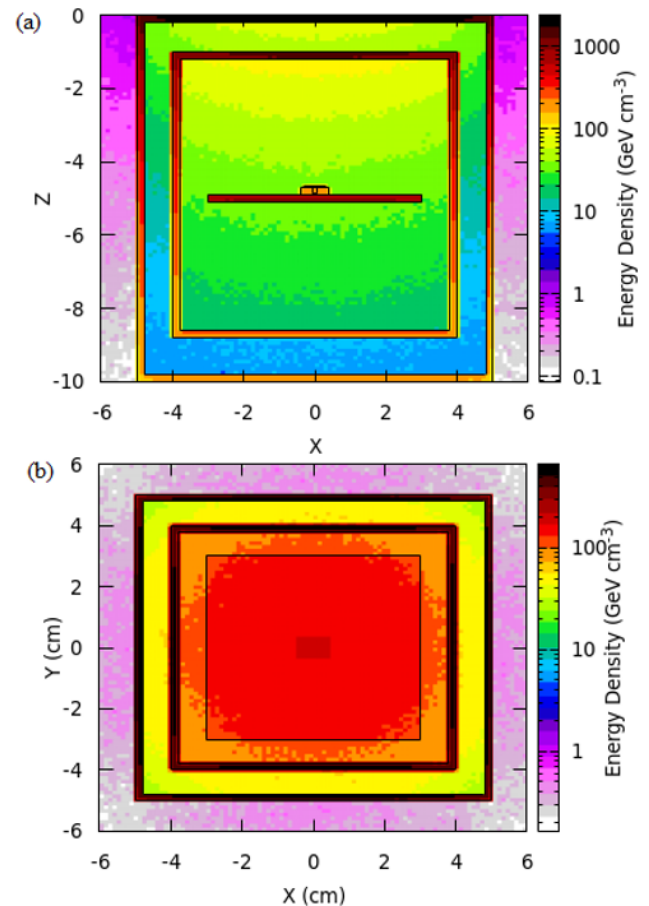


Fig. 8 Simulated energy deposition of the neutrons from FNG on the CubeSat. Fig. 8. (a) shows the axial interaction of the neutrons (coming from the upper part of the figure) with the satellite. Fig. 8. (b) is a sketch of the integral dose in the radial direction.

E. Comparison of the simulated response

The SIIMEVNE fluence allows comparing damages level imparted from different kinds of particles. Using the distributed facility, we can reproduce equivalent damages of days or years (according to the selected beam) of exposure to the orbital conditions in one hour of irradiation. The response difference between doses on radFET and the PCB card depends on the irradiation geometry (positions and beam spot sizes) that are not controlled in the orbital conditions. Tab. IV reports a comparison between the Van Allen dose rate and the simulated ones acquired during the irradiation in the distributed facility. To compare the damages from different particles the values of the corresponding SIIMEVNE fluences are reported.

TABLE IV
COMPARISON OF THE SIMULATED IRRADIATIONS

Radiative source	Dose Rate to radFET active part	Dose Rate on PCB card	SIIMEVNE fluence on PCB Card after 1-hour irradiation	Years of equivalent damage in orbital condition to the PCB card
	rad/day	rad/day	p/cm ²	
TOP_IMPLART @ 1 nA	962.57	145.75	7.67×10^{10}	2.32 years
REX @ 1 μA	14544	1494	6.64×10^{13}	2005 years
FNG ($1 \times 10^9 \text{ s}^{-1}$)	4.7×10^{-4}	3.2×10^{-3}	7.07×10^9	77.93 days
TAPIRO (1kW)	155.4	0.366	8.83×10^{11}	26.67 years
Van Allen belt	7.7	9.3×10^{-4}	3.78×10^6	

The estimated dose rates to the radFET grow proportionally to the intensity of the particle fluxes and the equivalent damages fluences grow accordingly.

As reported in Table IV, it is apparent that all the considered facilities greatly outperform the equivalent damages fluences of the orbital source term imparted to the PCB card. The greater effect is obtained using the electrons from the REX accelerator. To confirm the estimated trend work is in progress to realize the homologous experiments in each facility. Probably, besides the radFET the use of dedicated sensors for measuring the Non-Ionizing Energy Loss (NIEL) could be planned. In this manner, we will have direct and indirect confirmation of the facilities' performance.

V. CONCLUSIONS

This work was the first approach to consider the possibility of using ENEA irradiation facilities suite as a distributed laboratory to investigate the effect of mixed radiation fields. The irradiation for a CubeSat-like structure is the occasion to test the potential of such a distributed facility. The simulations show the possibility of obtaining damages equivalent to years of exposure to space radiation in our facility with a few hours of irradiation. Examining the energy range covered by our electron and proton accelerator, we found that the irradiations represent Low Earth Orbit radiation source terms and up to the Van Allen belt, where the contribution of GCR is not dominant. Future work will be addressed to refine some simulation models

like the FNG one. The second experimental phase has begun with the production of the prototypes of the satellites which will soon be irradiated. As a long-term activity, we will foresee the design and execution of similar experiments to European facilities with higher energetic particle output, and based on the experience gained, we will begin studying a national neutron spallation source and heavy ions accelerator to be located in one of the ENEA research centers.

REFERENCES

- [1] N. Burgio, et al. "Modelling the interaction of the Astro Bio Cube Sat with the Van Allen's Belt radiative field using Monte Carlo transport codes." *Radiation Detection Technology and Methods* 6.2 (2022): 262-279.
- [2] IAEA, 2017. Research Reactors for the development of materials and fuels for innovative nuclear energy systems, IAEA NUCLEAR ENERGY SERIES NO. NP-T5.8, International Atomic Energy Agency, Vienna, Austria.
- [3] J. W. G., Thomason, "The ISIS spallation neutron and muon source—the first thirty-three years." *Nuclear Instruments and Methods in Physics Research Section A: Accelerators, Spectrometers, Detectors and Associated Equipment* 917 (2019): 61-67.
- [4] J. Kohlbrecher., and W. Wagner. "The new SANS instrument at the Swiss spallation source SINQ." *Journal of applied crystallography* 33.3 (2000): 804-806.
- [5] T. E., Mason, et al. "The Spallation Neutron Source in Oak Ridge: A powerful tool for materials research." *Physica B: Condensed Matter* 385 (2006): 955-960.
- [6] Maekawa, Fujio, et al. "First neutron production utilizing J-PARC pulsed spallation neutron source JSNS and neutronic performance demonstrated." *Nuclear Instruments and Methods in Physics Research Section A: Accelerators, Spectrometers, Detectors and Associated Equipment* 620.2-3 (2010): 159-165.
- [7] https://www.enea.it/it/Ricerca_sviluppo/documenti/nucleare/TAPIRO.pdf
- [8] M. Martone, et al. *J. Nucl. Mat.* 212-215, 1661 (1994)
- [9] M. Angelone et al., *Rev. Sci. Instr.* **67**, 2189 (1996).
- [10] A. Pietropaolo et al. "The Frascati Neutron Generator: A multipurpose facility for physics and engineering", *IOP Conf. Series: Journal of Physics: Conf. Series* 1021 (2018) 012004, doi:10.1088/1742-6596/1021/1/012004.
- [11] E. Rhodes, C.E. Dickerman, A. De Volpi, C.W. Peters, *IEEE Trans. Nucl. Sci.* 39, 1041 (1992).
- [12] V. Surrenti et al. *Proc. 14th International Particle Accelerator Conference*, 2394-2397, TUPM092 (2023), doi:10.18429/jacow-ipac2023-tupm092
- [13] M. Vadrucchi et al., *Nuclear Inst. and Methods in Physics Research*, A 930 (2019) 126–131.
- [14] A. Holmes-Siedle, and L. Adams. "RADFET: A review of the use of metal-oxide-silicon devices as integrating dosimeters." *International Journal of Radiation Applications and Instrumentation. Part C. Radiation Physics and Chemistry* 28.2 (1986): 235-244.
- [15] G. Battistoni, et al. "Overview of the FLUKA code." *Annals of Nuclear Energy* 82 (2015): 10-18.
- [16] N. Burgio, "Radiometric impact assessments and shielding of CubeSat class satellites in interaction with orbital radiation fields and representativity of the calibration procedure and radiation damage tests in the ground facility." PhD thesis, DIAEE, Sapienza University of Rome, Rome, Italy, 2023.
- [17] N. Burgio, private communication, April 2023.
- [18] <https://www.varadis.com/products/>
- [19] <http://www.tscsrl.net/Home.html>
- [20] N. Burgio, et al. "Monte Carlo simulation analysis of integral data measured in the SCK-CEN/ENEA experimental campaign on the TAPIRO fast reactor. experimental and calculated data comparison." *Nuclear Engineering and Design* 273 (2014): 350-358.